

$^{40}\text{Ar}/^{39}\text{Ar}$ Geochronology Results for the Koosharem and Sigurd Quadrangles, Utah

by

Utah Geological Survey and New Mexico Geochronology Research Laboratory

Bibliographic citation for this data report:

Utah Geological Survey and New Mexico Geochronology Research Laboratory, 2019, $^{40}\text{Ar}/^{39}\text{Ar}$ geochronology results for the Koosharem and Sigurd quadrangles, Utah: Utah Geological Survey Open-File Report 709, variously paginated, <https://doi.org/10.34191/OFR-709>.



OPEN-FILE REPORT 709
UTAH GEOLOGICAL SURVEY

a division of

UTAH DEPARTMENT OF NATURAL RESOURCES

2019

STATE OF UTAH

Gary R. Herbert, Governor

DEPARTMENT OF NATURAL RESOURCES

Brian C. Steed, Executive Director

UTAH GEOLOGICAL SURVEY

R. William Keach II, Director

PUBLICATIONS

contact

Natural Resources Map & Bookstore

1594 W. North Temple

Salt Lake City, UT 84116

telephone: 801-537-3320

toll-free: 1-888-UTAH MAP

website: utahmapstore.com

email: geostore@utah.gov

UTAH GEOLOGICAL SURVEY

contact

1594 W. North Temple, Suite 3110

Salt Lake City, UT 84116

telephone: 801-537-3300

website: geology.utah.gov

INTRODUCTION

This Open-File Report makes available raw analytical data from laboratory procedures completed to determine the age of rock samples collected during geologic mapping funded or partially supported by the Utah Geological Survey (UGS). The reference listed in table 1 provides additional information regarding the geologic setting and significance or interpretation of the samples in the context of the area in which they were collected. This report was prepared by the New Mexico Geochronology Research Laboratory under contract to the UGS. These data are highly technical in nature and proper interpretation requires considerable training in the applicable geochronologic techniques.

Table 1. Sample numbers and locations.

Sample #	7.5' quadrangle	Easting	Northing	Reference
		UTM NAD83	UTM NAD83	
KO111417-9	Koosharem	416885	4273484	Doelling and others (in prep.)
KO111417-11	Koosharem	415497	4265048	Doelling and others (in prep.)
SG111417-1	Sigurd	413994	4293518	Doelling and others (in prep.)

DISCLAIMER

This open-file release is intended as a data repository for information gathered in support of various UGS projects. The data are presented as received from New Mexico Geochronology Research Laboratory and do not necessarily conform to UGS technical, editorial, or policy standards; this should be considered by an individual or group planning to take action based on the contents of this report. The Utah Department of Natural Resources, Utah Geological Survey, makes no warranty, expressed or implied, regarding the suitability of this product for a particular use. The Utah Department of Natural Resources, Utah Geological Survey, shall not be liable under any circumstances for any direct, indirect, special, incidental, or consequential damages with respect to claims by users of this product.

REFERENCE

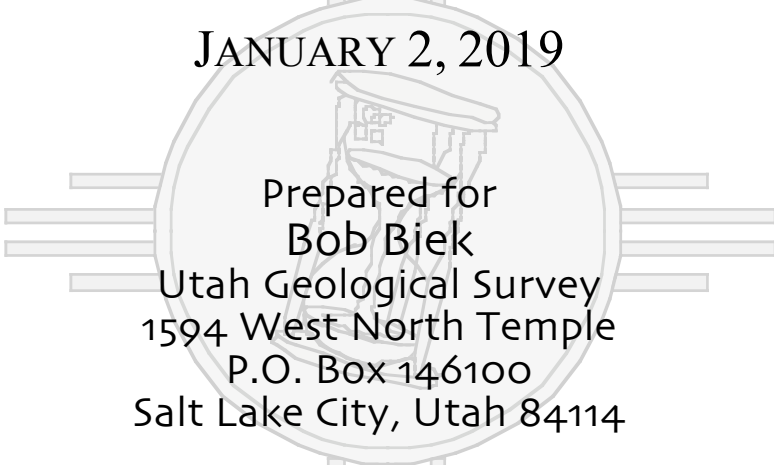
Doelling, H.H., Willis, G.C., and Kuehne, P.A., in preparation, Interim geologic map of the west half of the Salina 30' x 60' quadrangle, Sevier, Emery, and Piute Counties, Utah: Utah Geological Survey Open-File Report, scale 1:62,500.

$^{40}\text{Ar}/^{39}\text{Ar}$ Geochronology Results from the Marysvale Volcanic Field

By

Lisa Peters

JANUARY 2, 2019



Prepared for
Bob Biek
Utah Geological Survey
1594 West North Temple
P.O. Box 146100
Salt Lake City, Utah 84114

NEW MEXICO
GEOCHRONOLOGY RESEARCH LABORATORY
(NMGRL)

CO-DIRECTORS

DR. MATTHEW T. HEIZLER

DR. WILLIAM C. MCINTOSH

LABORATORY TECHNICIAN

LISA PETERS

Internal Report #: NMGRL-IR-1122

Introduction

Four samples were submitted for dating by the Utah Geological Survey. One was a basaltic andesite of unknown stratigraphic position, another a basaltic andesite lava or dense ashflow tuff and two volcanic units interpreted as post-caldera infilling. Groundmass concentrate was prepared from SG1114177-1 and KO111417-9 and sanidine was separated from KO111417-11. We were unable to prepare a sanidine separate from KO111417-12.

⁴⁰Ar/³⁹Ar Analytical Methods and Results

The groundmass concentrate was prepared from the basalt by crushing and choosing fragments visibly free of phenocrysts. The tuff sample was crushed, washed in dilute hydrofluoric acid, sieved and treated with density liquids and/or the magnetic separator and then the sanidine crystals hand-picked. The mineral separates and monitors (Fish Canyon tuff sanidine, 28.201, Kuiper et al., 2008) were loaded into aluminum discs and irradiated for 16 hours at the USGS TRIGA reactor in Denver Colorado.

The groundmass concentrates were step-heated with a defocused Photon Machines diode laser and analyzed with a Thermo Helix MCPlus mass spectrometer. The sanidine was fused with a Photon Machines CO₂ laser and analyzed with a Thermo Argus VI mass spectrometer. Abbreviated analytical methods for the dated samples are given in Table 1. The age results are summarized in Table 1 and the argon isotopic data are given in Tables 2 and 3.

Fifteen crystals of KO111417-11 were analyzed as fused single crystals. Four crystals yielded K/Ca values indicative of plagioclase and were eliminated from the age calculation and one slightly younger crystal of sanidine was also eliminated. The remaining ten crystals yielded an age of 23.09±0.03 Ma (Figure 1).

The groundmass concentrates from samples SG111417-1 and KO111417-9 yielded similar age spectra with initially young apparent ages in the first few percent of the spectra that climb to a maximum and then decrease to a final flat section of the age

spectrum. This final flat portion of SG111417-1 contains 26.4% of the gas released and yields an age of 25.14 ± 0.05 Ma. The radiogenic yields increase uniformly from 28.2% to 89.0% over 90.5 % of the age spectrum. From that point to the end of the age spectrum, the radiogenic yields decrease gently to 86.2%. The flat portion of KO111417-9 contains the final 28.8% of the gas released and yields an age of 24.29 ± 0.02 Ma. The radiogenic yields increase rapidly from a low of 9.7% to 99.6% over the initial 43.9% of the gas released and then remain fairly constant over the remainder of the spectrum, decreasing only slightly to 94.8%.

Discussion

We feel the age assigned to KO111417-11 (23.09 ± 0.03 Ma) provides a precise, reliable eruption age for the unit referred to as Tsf of Rowley.

The age spectra from samples SG111417-1 and KO111417-9 do not provide data that is as straightforward. Complex basalt age spectra can result from a variety of processes that can lead to somewhat ambiguous interpretations. The basaltic andesite samples dated here have initially young ages for the first few percent of the spectra that climb to a maximum before declining to an overall flat section for the last several heating steps. ^{39}Ar recoil can impact samples like basalts that are comprised of multiple phases of variable K content. During irradiation, recoil displaces ^{39}Ar on the order of $0.1 \mu\text{m}$ and thus relatively high K phases can be slightly depleted in ^{39}Ar that is implanted into neighboring relatively low K phases. Depending on the temperature that these variable phases degas during step heating, there can be complexities in the age spectra that are not a result of geological processes. For instance, if a low K phase that has received ^{39}Ar degasses during the initial steps, its apparent age will be reduced whereas the phase that has been depleted in ^{39}Ar will have an anomalously high apparent age. Combined, this can lead to a spectrum with initially young ages followed by older apparent ages relative to the true eruption age (similar to the spectra from this study). However, the high-K groundmass of a basalt will generally dominate the early gas release and thus in the case of these basalts, it is unlikely that the initially young ages are due to ^{39}Ar recoil. ^{39}Ar can also be ejected from the sample during irradiation and this will cause the apparent age to

be too old and thus it is possible that the high initial ages of the spectra that decline for later heating steps could result from recoil ejection of phases that degas at low temperature and that have also lost ^{39}Ar due to recoil.

In addition to recoil, anomalously young apparent ages can be related to radiogenic ^{40}Ar loss, caused by reheating and/or alteration, but older apparent ages can be related to incorporation of excess argon (i.e. initial argon that is trapped in the sample that has a $^{40}\text{Ar}/^{36}\text{Ar}$ value greater than the atmospheric value of 295.5). Excess argon can sometimes be detected on an isochron diagram and manifest itself by a correlation of decreasing radiogenic yields and increasing apparent ages such as exhibited by sample SC111417-1 (Fig 2a). Steps D-G clearly show this relationship and when plotted on an isochron diagram yield a linear array that projects to a trapped initial $^{40}\text{Ar}/^{36}\text{Ar}$ value of 321 ± 7 and an apparent age of 24.92 ± 0.10 Ma (isochron fig 2c). Steps H-M have consistent ages with a weighted mean of 25.14 ± 0.05 Ma and also fairly constant radiogenic argon values. Because there is only minor spread in radiogenic yield of these steps, the data cluster on an isochron diagram and lead to a fairly imprecise isochron age of 25.0 ± 0.4 Ma with a trapped initial component within error of atmosphere. Thus a possible interpretation of this complex spectrum is that it contains multiple trapped components (cf. Heizler et al., 1988) that are thermally distinct during degassing of the sample. Sample K0100417-9 displays a similar age spectrum pattern, but has high and constant radiogenic yields that make isochron analysis relatively meaningless. The initially old ages could be contaminated with excess argon, but due to limited data spread it cannot be readily detected on the isochron.

Although effects of recoil cannot be unambiguously evaluated, our preferred interpretation is that the down stepping pattern of ages on the age spectrum is related to early degassing of an excess ^{40}Ar component that is exhausted at higher temperatures. These higher temperature steps therefore contain an atmospheric component and thus reveal a flat segment on the age spectrum. Thus our preferred eruption age is provided by the weighted mean age of the high temperature steps as shown in Fig 2.

References Cited

- Heizler, M.T., Lux, D.R. and Decker, E.R., 1988, The age and cooling history of the Chain of Ponds and Big Island Pond plutons and the Spider Lake Granite, west-central Maine and Quebec: *Amer. J. Science*, v. 288, p.925-952.
- Kuiper, K. F., Deino, A., Hilgen, F. J., Krijgsman, W., Renne, P. R., and Wijbrans, J. R., 2008, Synchronizing rock clocks of earth history: *Science*, v. 320, p. 500-504.
- Min, K., Mundil, R., Renne, P. L., and Ludwig, K.R., 2000, A test for systematic errors in $^{40}\text{Ar}/^{39}\text{Ar}$ geochronology through comparison with U/Pb analysis of a 1.1-Ga rhyolite: *Geochimica et Cosmochimica Acta*, v. 64, p. 73-98.
- Taylor, J.R., 1982. *An Introduction to Error Analysis: The Study of Uncertainties in Physical Measurements*, Univ. Sci. Books, Mill Valley, Calif., 270 p.

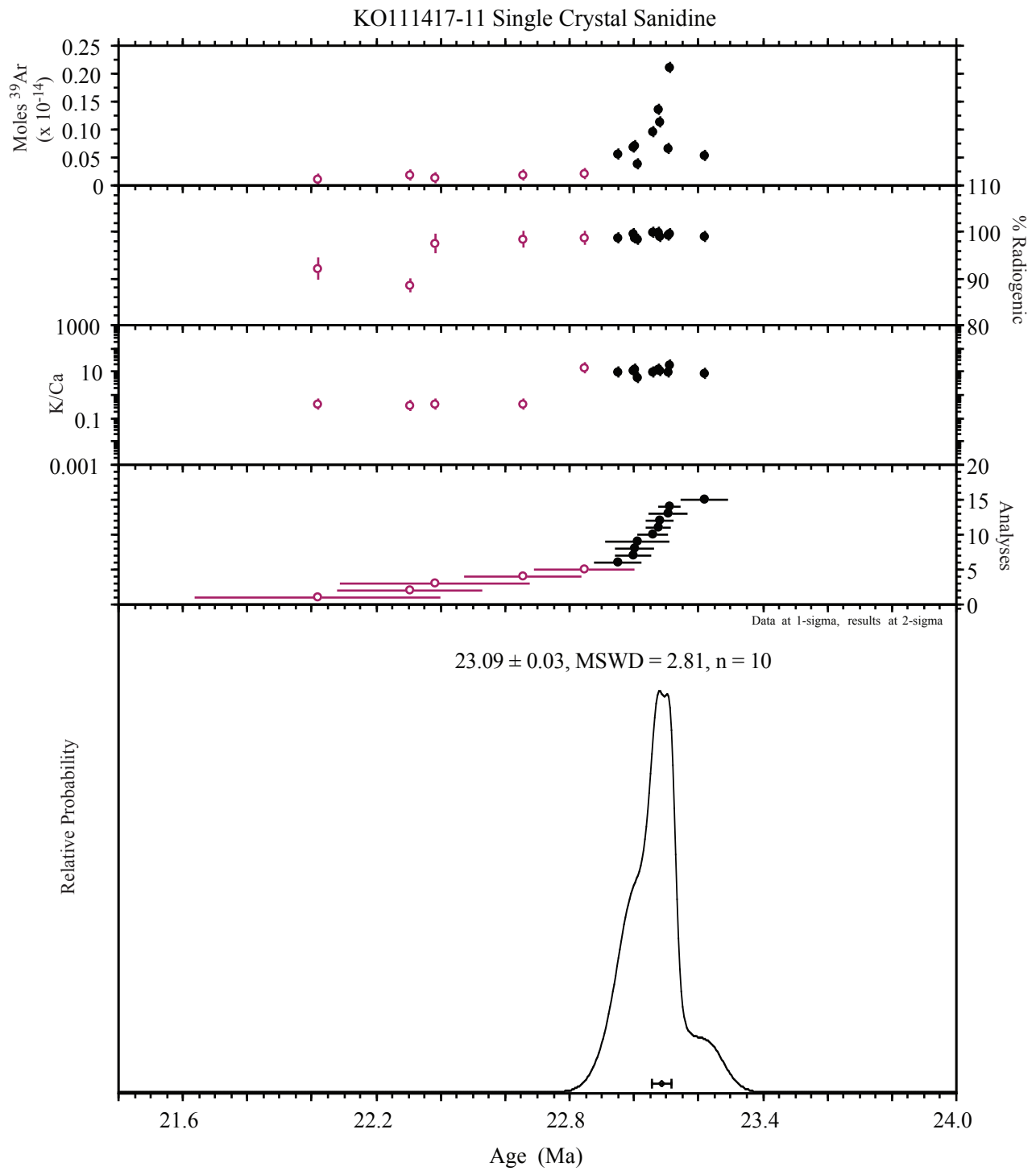


Figure 1 . Age probability distribution diagram of KO111417-11 sanidine.

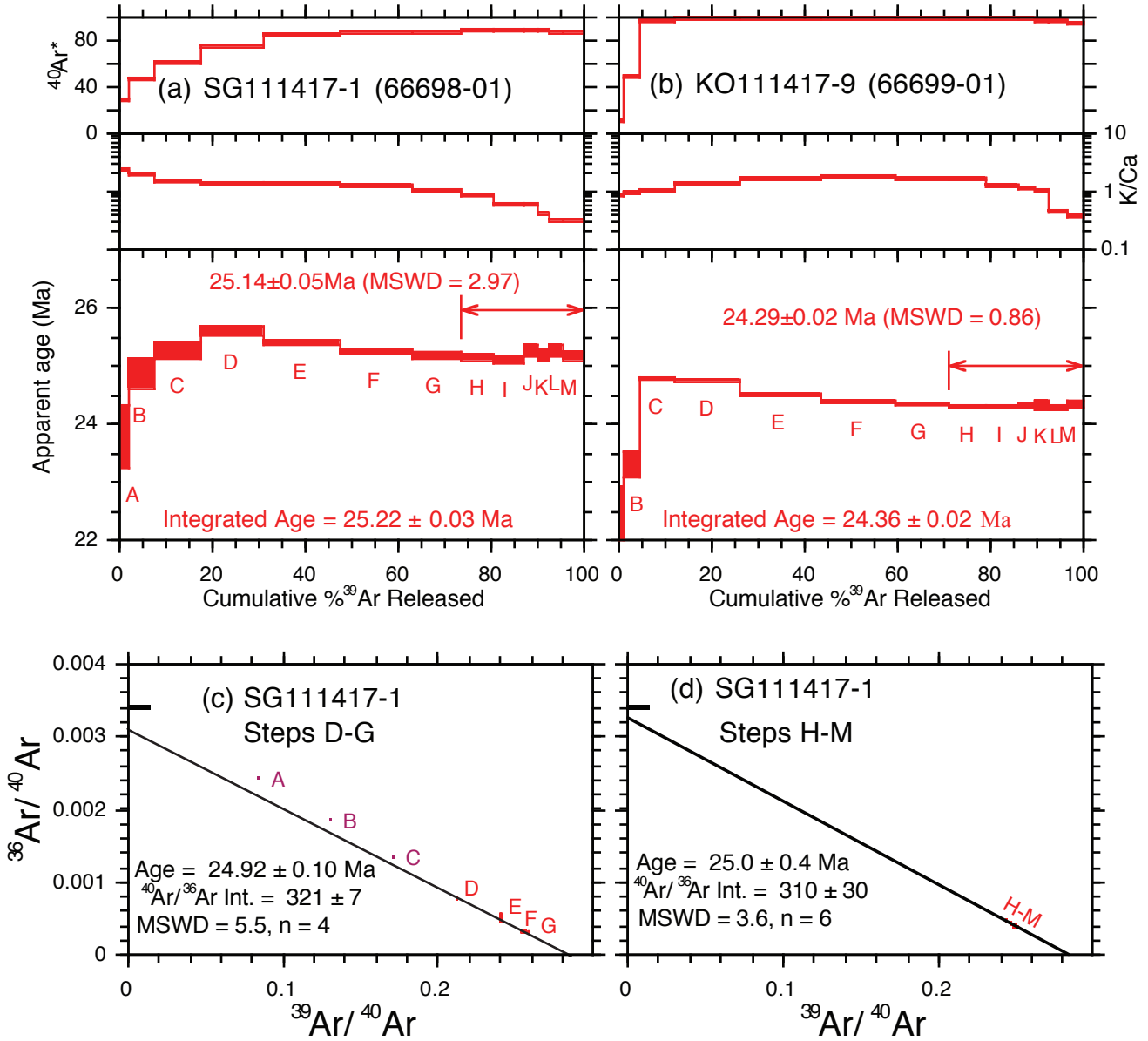


Figure 2. Age spectrum and isochron for SG111417-1 (a) and age spectrum for KO111417-9 (b).

Table 1. Summary of $^{40}\text{Ar}/^{39}\text{Ar}$ results and analytical methods

Sample	Lab #	Irradiation	mineral	age analysis	steps/analyses	Age	$\pm 2\sigma$	MSWD	comments
KO111417-11	66658	300	sanididne	single crystal total fusion	10	23.09	0.03	2.81	
SG111417-1	66698	300	groundmass concentrate	bulk step-heat	6	25.14	0.05	2.97	
KO111417-9	66699	300	groundmass concentrate	bulk step-heat	6	24.29	0.02	0.86	

Sample preparation and irradiation:

Minerals separated with standard heavy liquid, Franz Magnetic and hand-picking techniques.

Samples in NM-300 irradiated in a machined Aluminum tray for 16 hours in C.T. position, USGS TRIGA, Denver, Colorado.

Neutron flux monitor Fish Canyon Tuff sanidine (FC-2). Assigned age = 28.201 Ma (Kuiper et al., 2008).

Instrumentation:

Total fusion analyses performed on a Argus VI mass spectrometer on line with automated all-metal extraction system. System = Jan

Step-heat analyses performed on a Helix MCPlus mass spectrometer on line with automated all-metal extraction system. System = Felix

Multi-collector configuration: 40Ar-H1, 39Ar-Ax, 38Ar-L1, 37Ar-L2, 36Ar-CDD

Flux monitors fused with a Photon Machines Inc. CO₂ laser. Alunites step-heated with a Photon Machine Inc. Diode laser.

Analytical parameters:

Sensitivity for the Helix MCPlus with the Diode laser (step-heated samples) is 3.75 e-16 moles/fA.

Sensitivity for the Argus VI with the CO₂ laser (fused monitors) is 4.00 e-17 moles/fA.

Typical system blank and background was 281.7, 1.53, 8.07, 7.53, 1.05 x 10⁻¹⁸ moles at masses 40, 39, 38, 37 and 36, respectively for the laser analyses.

J-factors determined by CO₂ laser-fusion of 6 single crystals from each of 8 radial positions around the irradiation tray.

Decay constants and isotopic abundances after Minn et al., (2000).

Table 2. $^{40}\text{Ar}/^{39}\text{Ar}$ analytical data.

ID	Power (watts)	$^{40}\text{Ar}/^{39}\text{Ar}$	$^{37}\text{Ar}/^{39}\text{Ar}$	$^{36}\text{Ar}/^{39}\text{Ar}$ ($\times 10^{-3}$)	$^{39}\text{Ar}_K$ ($\times 10^{-15}$ mol)	K/Ca	$^{40}\text{Ar}^*$ (%)	Age (Ma)	$\pm 1\sigma$ (Ma)
KO111417-11 , Sanidine, J=0.0039024 \pm 0.03%, IC=1.007472 \pm 0.0014438, NM-300B, Lab#=66658, Argus VI									
13	2.1	3.382	1.538	1.374	0.062	0.33	91.8	22.02	0.37
14	2.1	3.567	1.629	1.886	0.122	0.31	88.2	22.31	0.21
15	2.1	3.243	1.490	0.7118	0.083	0.34	97.3	22.39	0.28
12	2.1	3.250	1.499	0.6098	0.139	0.34	98.3	22.66	0.16
06	2.1	3.277	0.0386	0.1845	0.158	13.2	98.4	22.85	0.14
08	2.1	3.289	0.0563	0.1826	0.429	9.1	98.5	22.95	0.05
11	2.1	3.271	0.0529	0.0991	0.537	9.7	99.2	23.00	0.04
09	2.1	3.294	0.0473	0.1719	0.558	10.8	98.6	23.01	0.04
07	2.1	3.310	0.1094	0.2393	0.284	4.7	98.1	23.01	0.08
10	2.1	3.268	0.0620	0.0626	0.748	8.2	99.6	23.06	0.03
05	2.1	3.270	0.0464	0.0566	1.064	11.0	99.6	23.08	0.02
02	2.1	3.302	0.0516	0.1619	0.886	9.9	98.7	23.08	0.03
01	2.1	3.289	0.0630	0.1079	0.517	8.1	99.2	23.11	0.04
04	2.1	3.280	0.0305	0.0657	1.664	16.7	99.5	23.11	0.01
03	2.1	3.317	0.0690	0.1519	0.414	7.4	98.8	23.22	0.05
Mean age $\pm 2\sigma$			n=10	MSWD=2.81		9.5 \pm 6.2		23.09	0.03

Notes:

Isotopic ratios corrected for blank, radioactive decay, and mass discrimination, not corrected for interfering reactions.

Errors quoted for individual analyses include analytical error only, without interfering reaction or J uncertainties.

Mean age is weighted mean age of Taylor (1982). Mean age error is weighted error

of the mean (Taylor, 1982), multiplied by the root of the MSWD where MSWD>1, and also

incorporates uncertainty in J factors and irradiation correction uncertainties.

Decay constants and isotopic abundances after Min et al., (2000).

symbol preceding sample ID denotes analyses excluded from mean age calculations.

Ages calculated relative to FC-2 Fish Canyon Tuff sanidine interlaboratory standard at 28.201 Ma

Decay Constant (LambdaK (total)) = 5.543e-10/a

Correction factors:

$$(^{39}\text{Ar}/^{27}\text{Ar})_{\text{Ca}} = 0.000709 \pm 0.000006$$

$$(^{36}\text{Ar}/^{27}\text{Ar})_{\text{Ca}} = 0.0002818 \pm 0.0000005$$

$$(^{38}\text{Ar}/^{39}\text{Ar})_K = 0.01139$$

$$(^{40}\text{Ar}/^{39}\text{Ar})_K = 0.006385 \pm 0.0003$$

Table 3. $^{40}\text{Ar}/^{39}\text{Ar}$ analytical data.

ID	Power (Watts)	$^{40}\text{Ar}/^{39}\text{Ar}$	$^{37}\text{Ar}/^{39}\text{Ar}$	$^{36}\text{Ar}/^{39}\text{Ar}$ ($\times 10^{-3}$)	$^{39}\text{Ar}_K$ ($\times 10^{-15}$ mol)	K/Ca	$^{40}\text{Ar}^*$ (%)	^{39}Ar (%)	Age (Ma)	$\pm 1\sigma$ (Ma)
SG111417-1 , Groundmass, 18.91 mg, J=0.0039126 \pm 0.02%, IC=1.009946 \pm 0.003419, NM-300E, Lab#=66698-01, Argus VI										
Xi A	1.0	11.83	0.2113	28.78	11.0	2.4	28.2	2.1	23.76	0.27
Xi B	1.6	7.670	0.2619	14.19	28.9	1.9	45.6	7.5	24.85	0.13
Xi C	2.2	5.837	0.3309	7.814	53.3	1.5	60.9	17.6	25.25	0.07
Xi D	3.0	4.760	0.3611	4.018	71.8	1.4	75.7	31.1	25.58	0.04
Xi E	4.0	4.223	0.3717	2.306	88.6	1.4	84.6	47.9	25.37	0.02
Xi F	5.0	4.048	0.4141	1.793	82.2	1.2	87.7	63.4	25.23	0.02
Xi G	5.5	4.037	0.4934	1.809	54.1	1.0	87.8	73.6	25.17	0.02
H	6.0	4.015	0.6105	1.786	38.6	0.84	88.1	80.9	25.13	0.03
I	7.0	4.007	0.8335	1.854	34.8	0.61	88.0	87.5	25.07	0.03
J	8.0	3.990	0.8783	1.726	15.9	0.58	89.0	90.5	25.24	0.04
K	10.0	3.991	1.174	1.859	12.5	0.43	88.7	92.8	25.15	0.05
L	15.0	4.067	1.579	2.192	15.8	0.32	87.3	95.8	25.24	0.05
M	20.0	4.103	1.629	2.369	22.2	0.31	86.2	100.0	25.15	0.04
Integrated age $\pm 2\sigma$			n=13		529.7	0.93	K2O=2.75%		25.22	0.03
Plateau $\pm 2\sigma$ steps H-M			n=6	MSWD=2.97	139.866	0.574\pm0.401	26.4		25.14	0.05
Isochron$\pm 2\sigma$ steps H-M			n=6	MSWD=3.61		$^{40}\text{Ar}/^{36}\text{Ar}=310\pm 30$			25.01	0.42
KO111417-9 , Groundmass, 15.27 mg, J=0.0039099 \pm 0.01%, IC=1.009946 \pm 0.003419, NM-300E, Lab#=66699-01, Argus VI										
X A	1.0	30.94	0.6121	94.70	7.3	0.83	9.7	1.3	21.36	0.77
X B	1.6	6.682	0.5142	11.66	19.7	0.99	49.0	4.6	23.29	0.11
X C	2.2	3.628	0.4702	0.6028	44.9	1.1	96.2	12.4	24.76	0.02
X D	3.0	3.508	0.3740	0.1854	79.3	1.4	99.3	26.0	24.73	0.01
X E	4.0	3.463	0.2993	0.1344	104.0	1.7	99.6	43.9	24.48	0.01
X F	5.0	3.448	0.2815	0.1328	93.0	1.8	99.5	59.9	24.36	0.01
X G	5.5	3.452	0.2945	0.1744	65.6	1.7	99.2	71.2	24.31	0.01
H	6.0	3.459	0.3183	0.2127	46.6	1.6	98.9	79.3	24.29	0.01
I	7.0	3.475	0.3987	0.2995	39.3	1.3	98.4	86.0	24.27	0.01
J	8.0	3.485	0.4392	0.3329	21.7	1.2	98.2	89.8	24.30	0.02
K	10.0	3.555	0.4891	0.5845	17.7	1.0	96.3	92.8	24.30	0.03
L	15.0	3.547	1.070	0.7484	24.1	0.48	96.3	97.0	24.25	0.03
M	20.0	3.611	1.366	1.017	17.7	0.37	94.8	100.0	24.32	0.03
Integrated age $\pm 2\sigma$			n=13		581.0	1.2	K2O=3.74%		24.36	0.02
Plateau $\pm 2\sigma$ steps H-M			n=6	MSWD=0.86	167.144	1.118\pm0.953	28.8		24.29	0.02

Notes:

Isotopic ratios corrected for blank, radioactive decay, and mass discrimination, not corrected for interfering reactions.

Errors quoted for individual analyses include analytical error only, without interfering reaction or J uncertainties.

Integrated age calculated by summing isotopic measurements of all steps.

Integrated age error calculated by quadratically combining errors of isotopic measurements of all steps.

Plateau age is inverse-variance-weighted mean of selected steps.

Plateau age error is inverse-variance-weighted mean error (Taylor, 1982) times root MSWD where MSWD>1.

Plateau error is weighted error of Taylor (1982).

Decay constants and isotopic abundances after Min et al., (2000).

symbol preceding sample ID denotes analyses excluded from plateau age calculations.

Weight percent K₂O calculated from ³⁹Ar signal, sample weight, and instrument sensitivity.

Ages calculated relative to FC-2 Fish Canyon Tuff sanidine interlaboratory standard at 28.201 Ma

Decay Constant (LambdaK (total) = 5.463e-10/a

Correction factors:

$$(^{39}\text{Ar}/^{37}\text{Ar})_{\text{Ca}} = 0.000709 \pm 0.000006$$

$$(^{36}\text{Ar}/^{37}\text{Ar})_{\text{Ca}} = 0.0002818 \pm 0.0000005$$

$$(^{38}\text{Ar}/^{39}\text{Ar})_{\text{K}} = 0.01139$$

$$(^{40}\text{Ar}/^{39}\text{Ar})_{\text{K}} = 0.006385 \pm 0.0003$$
